Investigating the Role of the Outer-Coordination Sphere in [Ni(P$^{Ph}_2$N$^{Ph-R}_2$)$_2$]$^{2+}$ Hydrogenase Mimics

Avijita Jain, Matthew L. Reback, Mary Lou Lindstrom, Colleen E. Thogerson, Monte L. Helm, Aaron M. Appel, and Wendy J. Shaw*

Chemical and Materials Sciences Division, Pacific Northwest National Laboratory, Richland, Washington 99354, United States

S Supporting Information

ABSTRACT: A series of dipeptide substituted nickel complexes with the general formula, [Ni-(P$^{Ph}_2$N$^{NNA-amino\ acid/ester}_2$)$_2$](BF$_4$)$_2$, have been synthesized and characterized (P$_2$N$_2$ = 1,5-diaza-3,7-diphosphacyclooctane, and the dipeptide consists of the non-natural amino acid, 3-(4-aminophenyl)propionic acid (NNA), coupled to amino acid/esters = glutamic acid, alanine, lysine, and aspartic acid). Each of these complexes is an active electrocatalyst for H$_2$ production. The effects of the outer-coordination sphere on the catalytic activity for the production of H$_2$ were investigated; specifically, the impact of sterics, the ability of the side chain or backbone to protonate and the pK_a values of the amino acid side chains were studied by varying the amino acids in the dipeptide. The catalytic rates of the different dipeptide substituted nickel complexes varied by over an order of magnitude. The amino acid derivatives display the fastest rates, while esterification of the terminal carboxylic acids and side chains resulted in a decrease in the catalytic rate by 50−70%, implicating a significant role of protonated sites in the outer-coordination sphere on catalytic activity. For both the amino acid and ester derivatives, the complexes with the largest substituents display the fastest rates, indicating that catalytic activity is not hindered by steric bulk. These studies demonstrate the significant contribution that the outer-coordination sphere can have in tuning the catalytic activity of small molecule hydrogenase mimics.
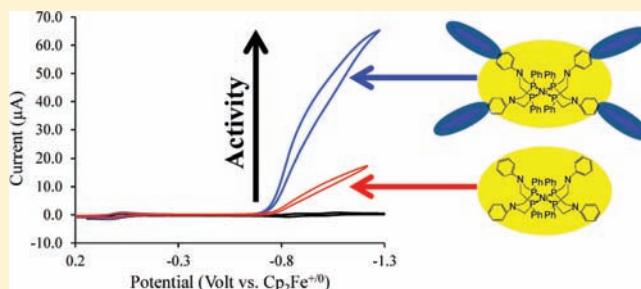
INTRODUCTION

Studies of hydrogenase enzymes have revealed that inexpensive metals like nickel and iron are capable of catalyzing the oxidation and production of H$_2$ with high catalytic rates (10 000 s^{-1}) and low overpotentials (<100 mV), properties that are needed for storage and subsequent use of energy from renewable sources.[1−5] In the active site of the [FeFe]-hydrogenase enzyme, a nitrogen base in an azadithiolate ligand positioned near the distal iron atom is thought to be critical to hydrogenase activity by mediating proton transfer to and from the active site (**1**).[3,6] This prompted studies in molecular mimics, such as [Ni(P$^R_2$N$^{R'}_2$)$_2$]$^{2+}$, (**2**) which have shown that the incorporation of a pendant amine (proton relay) resulted in rate enhancements of 2−3 orders of magnitude, with derivatives surpassing the rates of hydrogenase enzymes, although at higher overpotentials.[7−21]
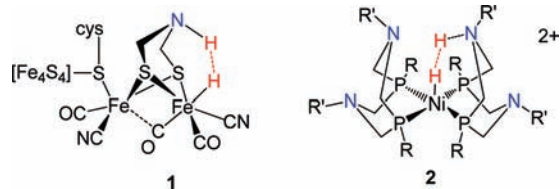
It has been shown that the outer-coordination sphere (the protein matrix surrounding the active site) in hydrogenases plays an essential role in catalysis by controlling the transfer of H$_2$ gas,

protons, and electrons[1−3] and may also control the environmental conditions around the active site by positioning hydrophobic, hydrophilic, or charged residues. Our recent investigation on the incorporation of amino acids and dipeptides into a hydrogenase functional mimic, [Ni(P$^{Ph}_2$N$^{Ph}_2$)$_2$]$^{2+}$, showed that the outer-coordination sphere can also influence the catalytic activity of molecular catalysts.[22] Coupling amino acids and dipeptides to the para position of the N-phenyl ring of this complex gave [Ni(P$^{Ph}_2$N$^{Ph-aminoacid/dipeptide}_2$)$_2$]$^{2+}$ and resulted in hydrogen production rates both faster and slower than the parent complex, varying by almost an order of magnitude for the four derivatives studied. Likewise, the addition of a phosphonate group in the same position resulted in a catalytic rate 2.5 times higher than that observed for the parent complex.[13] While these subtle modifications remote from the active site were not anticipated to influence catalysis to this degree, tuning of the active site in enzymes uses interactions over similar distances.

Due to the significant influence of the incorporation of single amino acids and dipeptides over catalytic rates, a more thorough understanding of the effects of individual amino acid functionalities on catalytic activity is needed before investigating the role of structured peptides with multiple functionalities. To this end, we have expanded upon our previous studies by
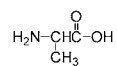
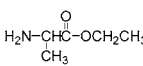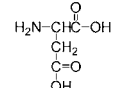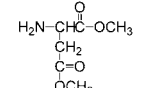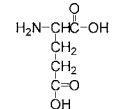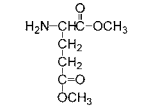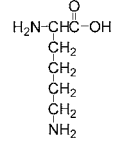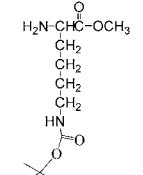incorporating dipeptides containing acidic, basic, and neutral amino acids, along with the corresponding esters, into the complexes, $[Ni(P^{Ph}_2N^{NNA}_2)_2]^{2+}$, where NNA is the non-natural amino acid, 3-(4-aminophenyl)propionic acid. This series of complexes allows us to investigate the impact of sterics, the ability of the side chains and backbone to protonate, and the pK_a of the amino acid side chain on the hydrogen production activity of $[Ni(P^{Ph}_2N^{NNA\text{-amino acid/ester}}_2)_2]^{2+}$. Herein, we describe the synthesis and characterization of eight new dipeptide containing complexes, including the amino acids—lysine (Lys), glutamic acid (Glu), aspartic acid (Asp), and alanine (Ala)—and the corresponding amino esters—lysine butyloxycarbonyl methyl ester (Lys(Boc)OMe), glutamic acid dimethyl ester (Glu-(OMe)OMe), aspartic acid dimethyl ester (Asp(OMe)OMe), and alanine ethyl ester (AlaOEt) (Table 1). The hydrogen production activities of the resulting complexes were investigated to evaluate the contribution of different properties of the outer-coordination sphere on the rates of hydrogen production.

■ MATERIALS AND METHODS

General Procedures. Electrospray ionization (ESI) and CI mass spectra were collected at the Indiana University Mass Spectrometry Facility on a Waters/Micromass LCT Classic using anhydrous solvents and inert atmosphere techniques. MALDI-MS were collected on a

Table 1. Amino Acids and Esters (R) Coupled through the Terminal Amine to the Carboxylate Group of $[Ni(P^{Ph}_2N^{NNA}_2)_2]^{2+}$ (Shown Here, Where R = OH) to Make Eight New Dipeptide $[Ni(P^{Ph}_2N^{NNA\text{-amino acid/ester}}_2)_2]^{2+}$ Complexes

Amino acid	Amino Ester
Alanine (Ala)	Alanine ethyl ester (AlaOEt)
Aspartic acid (Asp)	Aspartic acid dimethyl ester (Asp(OMe)OMe)
Glutamic acid (Glu)	Glutamic acid dimethyl ester (Glu(OMe)OMe)
Lysine (Lys)	Lysine butyloxycarbonyl methyl ester (Lys(Boc)OMe)

Waters LR used in reflectron mode, with alpha-cyano-4-hydroxycinnamic acid as the matrix, at the Protein Chemistry Technology Center, University of Texas, Dallas, TX. All experiments were carried out using standard Schlenk or inert-atmosphere glovebox techniques.

Synthesis and Materials. Materials were purchased commercially and used as received unless otherwise noted. Acetonitrile was purchased from Alfa Aesar and diethyl ether from Honeywell Burdick & Jackson. Fmoc-amino acids on Wang resin (100−200 mesh, 1% cross-linked polystyrene beads functionalized with 4-benzyloxybenzyl alcohol) with a substitution level of 0.6−0.7 mmol/g were purchased from Advanced Chemtech. Solvents were dried using an Innovative Technology, Inc. PureSolv solvent purification system. Water was dispensed from a Millipore Milli-Q purifier and degassed with nitrogen. Dimethylformamide trifluoromethanesulphonic acid, HDMF+, was prepared using a previously published method.[23] The precursor, $PhP(CH_2OH)_2$, was prepared by reacting 1 equiv of $PhPH_2$ with 2 equiv of p-formaldehyde, as previously described.[8] The ligands $P^{Ph}_2N^{NNA}_2$ and $P^{Ph}_2N^{NNE}_2$ (NNA = 3-(4-aminophenyl)propionic acid, NNE = ethyl 3-(4-aminophenyl)-propionoate), and the metal complex, $[Ni(CH_3CN)_6](BF_4)_2$, were prepared using previously published methods.[22,24]

General Synthetic Procedures. *$[Ni(P^{Ph}_2N^{NNA\text{-Glu}}_2)_2](BF_4)_2$ (Glu = Glutamic Acid).* The complex, $[Ni(P^{Ph}_2N^{NNA\text{-Glu}}_2)_2](BF_4)_2$, was synthesized using solid-phase peptide synthesis on a Wang resin. The fluorenyl methoxy carbonyl (FMOC) group was removed from FMOC-L-glutamic acid substituted Wang resin (1.0 g, 0.57 mmol) by stirring it with 20 mL of 20% piperidine in N-methylpyrrolidinone (NMP). The solid was rinsed with NMP and CH_2Cl_2 and collected by filtration. This process was repeated in order to achieve complete FMOC removal. The ligand, $P^{Ph}_2N^{NNA}_2$ (0.170 g, 0.285 mmol), dimethyl amino pyridine (DMAP) (0.069 g, 0.57 mmol), and diisopropyl carbodiimide (DIC) (60 μL, 0.57 mmol) were stirred for 15 min in 25 mL dichloromethane or until it turned clear. The FMOC deprotected glutamic acid resin was added to the mixture, and the solution was stirred at room temperature for 19 h, followed by filtration and collection of the peptidyl resin. The resin was washed with 100 mL dichloromethane and 100 mL acetonitrile to remove unreacted DMAP and reaction byproducts. The resin obtained was suspended in 30 mL acetonitrile, and $[Ni(CH_3CN)_6]$-$(BF_4)_2$ (0.07 g, 0.142 mmol) was then added. The reaction mixture was stirred at room temperature for 5 days resulting in a red colored resin. The colorless solution was filtered using a medium frit, and the red solid was collected. To cleave the complex from the resin, a 5 mL mixture of TFA:TIS:H$_2$O (95:2.5:2.5) (where TFA = trifluoroacetic acid, TIS = triisopropylsilane) was added to the solid and stirred for 4 h. The resulting reaction mixture was filtered and the volume of the filtrate was reduced to 1−2 mL under vacuum. The product was then flash precipitated by addition of this solution to 60 mL of stirring diethyl ether. Yield: 0.14 g, 0.07 mmol, 50%. $^{31}P\{^1H\}$ NMR (6 M D$_2$O in CD$_3$CN): δ 3.91 (b). ^1H NMR (6 M D$_2$O in CD$_3$CN); δ 7.07, 7.24, 7.35, 7.50 (m, 40 H, Ar-H and CONH); 4.31 (s, 4H, αCH); 4.19 (b, 8H, PCH_2N); 3.89 (b, 8H, PCH_2N); 2.89 (b, 8H, PhCH_2); 2.54 (b, 8H, CH_2CO); 2.23 (b, 8H, βCH_2), 1.81 (s, 4H, γCH_{2a}), 1.42(s, 4H, γCH_{2b}). MALDI MS: m/z calcd for $[Ni(P^{Ph}_2N^{NNA\text{-Glu}}_2)_2]^{2+}$: 1770.37, found: $[Ni(P^{Ph}_2N^{NNA\text{-Glu}}_2)_2]^{2+}$, 1770.29.

$[Ni(P^{Ph}_2N^{NNA\text{-Asp}}_2)_2](BF_4)_2$ (Asp = Aspartic Acid). The complex, $[Ni(P^{Ph}_2N^{NNA\text{-Asp}}_2)_2](BF_4)_2$ was prepared in a manner analogous to that of $[Ni(P^{Ph}_2N^{NNA\text{-Glu}}_2)_2](BF_4)_2$, using aspartic acid substituted Wang resin (1.0 g, 0.6 mmol), ligand $P^{Ph}_2N^{NNA}_2$ (0.179 g, 0.3 mmol), DMAP (0.073 g, 0.6 mmol), DIC (63 μL, 0.6 mmol), and $[Ni(CH_3CN)_6](BF_4)_2$ (0.071 g, 0.15 mmol). Yield: 0.135 g, 0.07 mmol, 47%. $^{31}P\{^1H\}$ NMR (6 M D$_2$O in CD$_3$CN): δ 5.0 (b). ^1H NMR (6 M D$_2$O in CD$_3$CN) δ 7.12, 7.23, 7.38 (m, 40 H, Ar-H and CONH); 4.63 (s, 4H, αCH); 4.20 (b, 8H, PCH_2N); 3.86 (b, 8H, PCH_2N); 2.86 (b, 8H, PhCH_2); 2.73 (b, 8H, CH_2CO); 2.50 (b, 8H, βCH_2). MALDI MS: m/z calcd. for $\{[Ni(P^{Ph}_2N^{NNA\text{-Asp}}_2)_2](BF_4)\}^+$: 1801.48, found: $\{[Ni(P^{Ph}_2N^{NNA\text{-Asp}}_2)_2](BF_4)\}^+$, 1801.47.

$[Ni(P^{Ph}_2N^{NNA\text{-Ala}}_2)_2](BF_4)_2$ (Ala = Alanine). The complex, $[Ni(P^{Ph}_2N^{NNA\text{-Ala}}_2)_2](BF_4)_2$, was prepared in a manner analogous to that of $[Ni(P^{Ph}_2N^{Glu}_2)_2](BF_4)_2$ using alanine substituted Wang resin (1.0 g, 0.6 mmol), ligand $P^{Ph}_2N^{NNA}_2$ (0.179 g, 0.150 mmol), DMAP (0.073 g, 0.6 mmol), DIC (63 μL, 0.6 mmol), and $[Ni(CH_3CN)_6](BF_4)_2$ (0.071

g, 0.15 mmol). Yield: 0.142 g, 0.08 mmol, 55%. ^{31}P{^{1}H} NMR (6 M D$_2$O in CD$_3$CN): δ 5.0 (b). ^{1}H NMR (6 M D$_2$O in CD$_3$CN) δ 7.45, 7.29, 7.11, 6.9 (m, 40 H, Ar-*H* and CON*H*); 4.31 (s, 4H, αC*H*); 4.25 (b, 8H, PC*H$_2$*N); 3.91(b, 8H, PC*H$_2$*N); 2.53 (b, 8H, PhC*H$_2$*), 2.30 (d, 12H, C*H$_3$*). MALDI MS: *m/z* calcd. for [Ni(P$^{Ph}_2$N$^{NNA-Ala}_2$)$_2$]$^{2+}$: 1539.52, found: [Ni(P$^{Ph}_2$N$^{NNA-Ala}_2$)$_2$]$^{2+}$, 1539.58.

[Ni(P$^{Ph}_2$N$^{NNA-Lys}_2$)$_2$](BF$_4$)$_2$ *(Lys = Lysine).* The complex, [Ni-(P$^{Ph}_2$N$^{NNA-lys}_2$)$_2$](BF$_4$)$_2$, was prepared in a manner analogous to that of [Ni(P$^{Ph}_2$N$^{NNA-Glu}_2$)$_2$](BF$_4$)$_2$ using lysine substituted Wang resin (1.0 g, 0.7 mmol), ligand P$^{Ph}_2$N$^{NNA}_2$ (0.203 g, 0.35 mmol), DMAP (0.085 g, 0.7 mmol), DIC (0.73 μL, 0.35 mmol), and [Ni(CH$_3$CN)$_6$](BF$_4$)$_2$ (0.175 g, 0.083 mmol). Yield: 0.170 g, 0.08 mmol, 40%. ^{31}P{^{1}H} NMR (6 M D$_2$O in CD$_3$CN): δ 4.93 (b). ^{1}H NMR (6 M D$_2$O in CD$_3$CN): δ 7.12, 7.26, 7.37 (b, 40H, Ar–H and CON*H*); 4.30 (s, 4H, αC*H*); 4.25 (b, 8H, PC*H$_2$*N); 3.83(b, 8H, PC*H$_2$*N); 2.87 (t, 8H, C*H$_2$*CO); 2.85 (b, 8H, PhC*H$_2$*), 2.52 (b, 8H, εC*H$_2$*); 1.75 (s, 4H, βC*H$_{2a}$*), 1.65 (s, 4H, βC*H$_{2b}$*), 1.59 (b, 8H, γC*H$_2$*), 1.33 (s, 4H, δC*H$_2$*). ESI MS (CH$_3$CN): *m/z* calcd. for [Ni(P$^{Ph}_2$N$^{NNA-Lys}_2$)$_2$]$^+$: 1767.75, found: [Ni-(P$^{Ph}_2$N$^{NNA-Lys}_2$)$_2$]$^+$, 1767.52.

P$^{Ph}_2$N$^{NNA-AlaOEt}_2$ *(AlaOEt = Alanine Ethyl Ester).* The ligand, P$^{Ph}_2$N$^{NNA-AlaOEt}_2$, was prepared by addition of 1 equiv of P$^{Ph}_2$N$^{NNA}_2$ (150 mg, 0.25 mmol) to 2.2 equiv of DIPEA (71.1 mg, 0.552 mmol) in 20 mL of dichloromethane. The mixture was stirred for 20 min. A 2 equiv portion of 2-(1H-benzotriazole-1-yl)-1,1,3,3-tetramethyluronium tetrafluoroborate (TBTU) (161 mg, 0.502 mmol) was then added to the mixture containing P$^{Ph}_2$N$^{NNA}_2$ and diisopropylethyl amine (DIPEA). The mixture was stirred for 20 min, 2 equiv of DL-alanine ethyl ester hydrochloride was added (77.0 mg, 0.502 mmol), and the solution was stirred overnight at room temperature. The solution was extracted extensively with basic water to remove the chloride, and the organic phase was dried over anhydrous magnesium sulfate. The solution was then passed through Celite, and the solvent was removed under vacuum. The resulting yellow/white solid was washed with acetonitrile and recrystallized from diethyl ether. Yield: 0.08 g 0.1 mmol, 40%. ^{31}P{^{1}H} NMR (CDCl$_3$): δ −50.05 (s) ^{1}H NMR (CDCl$_3$): δ 7.60, 7.50, 7.48 (m, 10H, NAr-*H*); 7.05 (d 4H PAr-*H*); 6.66 (d, 4H, PAr*H*); 6.01 (d, 2H, CON*H*); 4.53 (m, 2H, αC*H*); 4.44 (t, 4H, PC*H$_2$*N); 4.16 (q, 4H, C*H$_2$*COO), 4.02 (dd, 4H, PC*H$_2$*N); 2.83 (m, 4H, C*H$_2$*CO); 2.44 (m, 4H, C*H$_2$*Ar); 1.28 (d, 6H, βC*H$_3$*); 1.26 (t, 6H, C*H$_3$*). MALDI MS: *m/z* calcd for P$^{Ph}_2$N$^{NNA-AlaOEt}_2$: 796.87, found: [P$^{Ph}_2$N$^{NNA-AlaOEt}_2$ − 2H$^+$], 794.51. Elem. anal. calcd. for C$_{44}$H$_{54}$N$_4$O$_{10}$P$_2$: C, 66.32; N, 7.03; H, 6.83. Found: C, 66.26; N, 7.07; H, 6.95.

P$^{Ph}_2$N$^{NNA-Glu(OMe)OMe}_2$ *(Glu(OMe)OMe = Glutamic Acid Dimethyl Ester).* The ligand, P$^{Ph}_2$N$^{NNA-Glu(OMe)OMe}_2$, was prepared in a manner analogous to that of P$^{Ph}_2$N$^{NNA-AlaOEt}_2$ by stirring 2 equiv of TBTU (269.7 mg, 0.84 mmol), 1 equiv of P$^{Ph}_2$N$^{NNA}_2$ (250 mg, 0.42 mmol), and 2.2 equiv of DIPEA (0.15 mL, 0.84 mmol) in 20 mL dichloromethane. The mixture was stirred for 20 min followed by addition of a solution of L-glutamic acid dimethyl ester hydrochloride (177.7 mg, 0.84 mmol) and DIPEA (0.15 mL, 0.84 mmol) in 10 mL CH$_2$Cl$_2$. Extraction of the desired ligand was analogous to that of P$^{Ph}_2$N$^{AlaOEt}_2$. Yield: 31 mmol, 274.2 mg, 75%. ^{31}P{^{1}H} NMR (CD$_2$Cl$_2$): δ −50.97 (s). ^{1}H NMR (CD$_2$Cl$_2$): δ 7.38, 6.96, 6.56 (m, 18H, Ar-*H*); 5.99 (s, 2H, CON*H*); 4.31 (d, 2H, PC*H$_2$*N); 3.93 (d, 4H, PC*H$_2$*N); 3.54 (s, 6H, COC*H$_3$*); 3.51 (s, 6H, COC*H$_3$*); 2.33 (t, 4H, PhC*H$_2$*); 2.70 (t, 4H, C*H$_2$*CO); 4.42 (s, 2H, αC*H*); 2.19 (s, 4H, βC*H$_2$*); 2.01 (s, 2H, γC*H$_{2a}$*); 1.79 (s, 2H, γC*H$_{2b}$*). MALDI MS: *m/z* calcd for P$^{Ph}_2$N$^{NNA-Glu(OMe)OMe}_2$: 912.36, found: [P$^{Ph}_2$N$^{NNA-Glu(OMe)OMe}_2$ − 2H$^+$], 910.71. Elem. anal. calcd. for C$_{48}$H$_{58}$N$_4$O$_{10}$P$_2$: C, 63.15; N, 6.40; H, 6.10. Found: C, 62.90; H, 6.26; N, 6.02.

P$^{Ph}_2$N$^{NNA-Lys(Boc)OMe}_2$ *(Lys(Boc)OMe =Lysine (Boc) Methyl Ester).* The ligand, P$^{Ph}_2$N$^{NNA-Lys(Boc)OMe}_2$, was prepared in a manner analogous to that of P$^{Ph}_2$N$^{NNA-AlaOEt}_2$ by using 1 equiv of P$^{Ph}_2$N$^{NNA}_2$ (150 mg, 0.25 mmol), 2 equiv of TBTU (160 mg, 0.5 mmol), 2.2 equiv of DIPEA (71.1 mg, 0.552 mmol), and lysine(Boc)methyl ester hydrochloride (149 mg, 0.5 mmol). Yield: 227 mg, 0.21 mmol, 84%. ^{31}P{^{1}H}NMR (CDCl$_3$): δ −47.00 (s). ^{1}H NMR (CDCl$_3$): δ 7.61, 7.49, 7.07, 6.66 (m, 18H, Ar-*H*); 6.02 (d, 2H, CON*H*); 4.73 (m, 2H N*H*COO); 4.52 (q, 2H, αC*H*); 4.45 (d, 4H, PC*H$_2$*); 4.03 (m, 4H, PC*H$_2$*); 3.64 (s, 3H, OC*H$_3$*); 2.98 (q, 4H, εC*H$_2$*); 2.85 (t, 4H, PhC*H$_2$*); 2.48 (t, 4H, C*H$_2$*CONH}; 1.72 (m, 4H,

γC*H$_2$*); 1.57 (m, 4H, δC*H$_2$*); 1.28 (m, 2H, βC*H$_a$*); 1.38 (m, 2H, βC*H$_b$*); 1.40 (s, 18H, C(C*H$_3$*)$_3$). MALDI MS: *m/z* calcd for P$^{Ph}_2$N$^{NNA-Lys(Boc)OMe}_2$, 1082.54, found: [P$^{Ph}_2$N$^{NNA-Lys(Boc)OMe}_2$ − H$^+$], 1081.25. Elem. anal. calcd. for C$_{58}$H$_{80}$N$_6$O$_{10}$P$_2$: C, 64.31; N, 7.76; H, 7.44. Found: C, 64.05; N, 7.56; H, 7.48.

P$^{Ph}_2$N$^{NNA-Asp(OMe)OMe}_2$ *(Asp(OMe)OMe = Aspartic Acid Dimethyl Ester).* The ligand, P$^{Ph}_2$N$^{NNA-Asp(OMe)OMe}_2$, was prepared in a manner analogous to that of P$^{Ph}_2$N$^{AlaOEt}_2$ by using 2 equiv of TBTU (161 mg, 0.502 mmol), 1 equiv of P$^{Ph}_2$N$^{NNA}_2$ (150 mg, 0.25 mmol), 2.2 equiv of DIPEA (71.1 mg, 0.552 mmol), and 2 equiv of aspartic acid dimethyl ester hydrochloride (99.1 mg, 0.5 mmol). Yield: 43.4 mg, 0.05 mmol 20%. ^{31}P{^{1}H} NMR (CDCl$_3$): δ −50.05 (s). ^{1}H NMR (CDCl$_3$): δ 7.63, 7.50 (m, 10H, NAr*H*); 7.05 (d 4H PAr*H*); 6.66 (d, 4H, PAr*H*); 6.46 (d, 2H, CON*H*); 4.86 (m, 2H, αC*H*); 4.44 (t, 4H, PC*H$_2$*N); 4.02 (d, 4H, PC*H$_2$*N); 3.62 (s, 6H OC*H$_3$*); 3.60 (s, 6, OC*H$_3$*); 3.03 (m, 4H, βC*H$_2$*); 2.85 (m, 4H, C*H$_2$*C*H$_2$*Ar); 2.48 (m, 4H, C*H$_2$*Ar). MALDI MS: *m/z* calcd for P$^{Ph}_2$N$^{NNA-Asp(OMe)OMe}_2$: 884.33, found: [P$^{Ph}_2$N$^{NNA-Asp(OMe)OMe}_2$ − 2H$^+$], 882.71. Elem. anal. calcd. for C$_{46}$H$_{54}$N$_4$O$_{10}$P$_2$: C, 62.44; H, 6.15; N, 6.33. Found: C, 62.22; H, 6.15; N, 6.38.

[Ni(P$^{Ph}_2$N$^{NNA-AlaOEt}_2$)$_2$](BF$_4$)$_2$. Solid P$^{Ph}_2$N$^{NNA-AlaOEt}_2$ (0.080 g, 0.1 mmol) and [Ni(CH$_3$CN)$_6$](BF$_4$)$_2$ (0.024 mg, 0.05 mmol) were stirred overnight in acetonitrile (20 mL) to give a red solution. The solution was filtered using a medium frit to remove small amounts of suspended impurities. The solvent was removed under vacuum, and the residue was dissolved in 2 mL acetonitrile. The product was then flash precipitated by addition to 60 mL of stirring diethyl ether and filtered using a medium frit. Yield: 0.78 g, 0.04 mmol, 85%. ^{31}P{^{1}H} NMR (CD$_3$CN): δ 5.23 (s). ^{1}H NMR (CD$_3$CN): δ 7.44, 7.31, 7.20 (m, 36H, Ar-*H*); 6.76 (d, 4H, CON*H*); 4.34 (m, 4H, αC*H*); 4.20 (d, 8H, PC*H$_2$*N); 4.10 (m, 8H, C*H$_2$*COO); 3.93 (d, 8H, PC*H$_2$*N); 2.93 (t, 8H, C*H$_2$*CONH); 2.52 (t, 8H, C*H$_2$*Ar); 1.30 (d, 12H, C*H$_3$*); 1.21 (t, 12H, C*H$_2$*C*H$_3$*). ESI MS (CH$_3$CN): *m/z* calcd for [Ni(P$^{Ph}_2$N$^{NNA-AlaOEt}_2$)$_2$]$^{2+}$: 1651.64, found: [Ni(P$^{Ph}_2$N$^{NNA-AlaOEt}_2$)$_2$]$^{2+}$, 1651.57. Elem. anal. calcd. for C$_{88}$H$_{108}$N$_8$O$_{12}$P$_4$B$_2$F$_8$Ni: C, 57.88; H, 5.96; N, 6.14. Found: C, 57.11; H, 5.99; N, 6.25.

[Ni(P$^{Ph}_2$N$^{NNA-Glu(OMe)OMe}_2$)$_2$](BF$_4$)$_2$. The complex, [Ni-(P$^{Ph}_2$N$^{NNA-Glu(OMe)OMe}_2$)$_2$](BF$_4$)$_2$, was prepared in a manner analogous to that of [Ni(P$^{Ph}_2$N$^{NNA-AlaOEt}_2$)$_2$](BF$_4$)$_2$ using P$^{Ph}_2$N$^{Glu(OMe)OMe}_2$ (0.120 g, 0.14 mmol) and [Ni(CH$_3$CN)$_6$](BF$_4$)$_2$ (0.035 mg, 0.07 mmol). Yield: 0.107 g, 0.05 mmol, 80%. ^{31}P{^{1}H} NMR (CD$_2$Cl$_2$): δ 5.29 (s). ^{1}H NMR (CD$_3$CN): δ 7.41, 7.32, 7.26, 7.16 (m, 36H, Ar-*H*); 6.77 (s, 4H, CON*H*); 4.20 (d, 8H, PC*H$_2$*N); 3.90 (d, 8H, PC*H$_2$*N); 3.65 (s, 12H, COC*H$_3$*); 2.52 (t, 8H, PhC*H$_2$*); 2.90 (t, 8H, C*H$_2$*CO); 4.38 (s, 4H, αC*H*), 2.33 (s, 8H, βC*H$_2$*), 2.08 (s, 4H, γC*H$_{2a}$*), 1.82 (s, 4H, γC*H$_{2b}$*), 3.61 (s, 12H, COC*H$_3$*). ESI MS (CH$_3$CN): *m/z* calcd for {[Ni-(P$^{Ph}_2$N$^{NNA-Glu(OMe)OMe}_2$)$_2$] + BF$_4$}$^+$: 1969.66, found: {[Ni-(P$^{Ph}_2$N$^{NNA-Glu(OMe)OMe}_2$)$_2$] + BF$_4$}$^+$, 1969.66.

[Ni(P$_2$^{Ph}N$^{NNA-Lys(Boc)OMe}_2$)$_2$](BF$_4$)$_2$. The complex, [Ni-(P$_2$^{Ph}N$^{NNA-Lys(Boc)OMe}_2$)$_2$](BF$_4$)$_2$, was prepared in a manner analogous to that of [Ni(P$^{Ph}_2$N$^{NNA-AlaOMe}_2$)$_2$](BF$_4$)$_2$ using P$^{Ph}_2$N$^{NNA-Lys(Boc)OMe}_2$ (0.120 g, 0.12 mmol) and [Ni(CH$_3$CN)$_6$](BF$_4$)$_2$ (0.028 g, 0.06 mmol). Yield: 0.107 g, 0.05 mmol, 80%. ^{31}P{^{1}H}NMR (CDCl$_3$): δ 4.0 (s). ^{1}H NMR (CD$_3$CN): δ 7.46, 7.39, 7.30, 7.27 (m, 36H, Ar-*H*); 6.77 (d, 4H, CON*H*); 5.26 (m, 4H N*H*COO); 4.30 (q, 4H, αC*H*); 4.64 (d, 8H, PC*H$_2$*); 4.29 (m, 4H, PC*H$_2$*); 3.61 (s, 6H, OC*H$_3$*); 2.91 (t, 8H, PhC*H$_2$*); 2.51 (t, 8H, C*H$_2$*CONH); 2.78 (q, 8H, εC*H$_2$*); 1.96 (m, 4H, γC*H$_{2a}$*); 1.70 (m, 4H, δC*H$_2$*); 1.60 (m, 4H, γC*H$_{2b}$*); 1.36 (s, 36 H, C(C*H$_3$*)$_3$); 1.40 (m, 4H, βC*H$_{2a}$*); 1.24 (m, 4H, βC*H$_{2b}$*). MALDI MS: *m/z* calcd for [Ni(P$^{Ph}_2$N$^{NNA-Lys(Boc)OMe}_2$)$_2$]$^{2+}$: 2224.04, found: [Ni-(P$^{Ph}_2$N$^{NNA-Lys(Boc)OMe}_2$)$_2$]$^{2+}$, 2224.02.

[Ni(P$^{Ph}_2$N$^{NNA-Asp(OMe)OMe}_2$)$_2$](BF$_4$)$_2$. The complex, [Ni-(P$^{Ph}_2$N$^{NNA-Asp(OMe)OMe}_2$)$_2$](BF$_4$)$_2$, was prepared in a manner analogous to that of [Ni(P$^{Ph}_2$N$^{NNA-AlaOMe}_2$)$_2$](BF$_4$)$_2$ using P$^{Ph}_2$N$^{NNA-Asp(OMe)OMe}_2$ (0.043 g, 0.051 mmol) and [Ni(CH$_3$CN)$_6$](BF$_4$)$_2$ (0.012 mg, 0.025 mmol). Yield: 0.035 g, 0.017 mmol, 68%. ^{31}P{^{1}H} NMR (CD$_3$CN): δ 5.3 (s). ^{1}H NMR (CD$_3$CN): δ 7.44, 7.33, 7.19 (m, 36H, Ar*H*); 6.91 (d, 4H, CON*H*); 4.76 (m, 4H, αC*H*); 4.26 (d, 8H, PC*H$_2$*N); 3.95 (d, 8H, PC*H$_2$*N); 3.64 (s, 12H OC*H$_3$*); 3.61 (s, 12, OC*H$_3$*); 2.92 (t, 8H, COC*H$_2$*); 2.87 (d, 8H, βC*H$_2$*); 2.53 (m, 8H, C*H$_2$*Ar). ESI MS

Scheme 1. Synthesis of the Ligands $P^{Ph}_2N^{NNA\text{-}amino\ acid}_2$ (Top) and $P^{Ph}_2N^{NNA\text{-}amino\ ester}_2$ (Bottom)^a
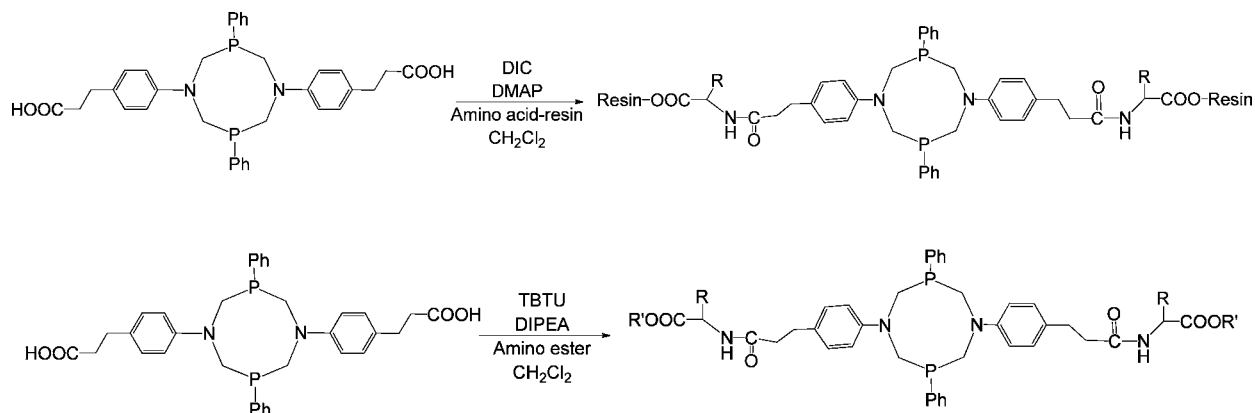
^{a}where R = amino acid/ester side chain and R′ = Me or Et.

(CH$_3$CN): m/z calcd for $[Ni(P^{Ph}_2N^{NNA\text{-}Asp(OMe)OMe}_2)_2]^{2+}$: 1827.60, found: $[Ni(P^{Ph}_2N^{NNA\text{-}Asp(OMe)OMe}_2)_2]^{2+}$, 1827.46.

NMR Studies. *Standard.* Solution state ^{1}H and ^{31}P NMR spectra were recorded on a Varian Inova or VNMRS spectrometer (500 or 300 MHz ^{1}H frequency). All ^{1}H chemical shifts were internally calibrated to the monoprotic solvent impurity. All ^{31}P{^{1}H}chemical shifts were externally referenced to phosphoric acid. Amino acid/ester containing metal complexes and ligands were characterized with ^{1}H–^{1}H TOCSY (mixing time = 80 ms) to fully assign the spectra and and ^{31}P–^{31}P EXSY (mixing time = 200 ms) to characterize exchange processes.

Structural Dynamics and pH Dependence. ^{31}P{^{1}H} NMR spectra were obtained overnight, at room temperature and at −40 °C, on solutions of 10 mM metal complex in *d*-acetonitrile containing 6 M water. Amino acid substituted nickel complexes were at pH = 2.5 under these conditions.

The pH of the solution was adjusted by addition of triethylamine to obtain a pH = 4.0 or trifluoroacetic acid to obtain a pH = 1.0.

Electrochemical Studies. All cyclic voltammetry experiments were carried out using a CH Instruments 1100A computer aided three-electrode potentiostat in a glovebox in 0.2 M Et$_4$N$^+$BF$_4$$^−$ acetonitrile solutions at scan rates of 100−1000 mV/s. The working electrode was a glassy carbon disk, and the counter electrode was a glassy carbon rod. A silver wire (amino acid containing Ni complexes) or a platinum wire (amino ester containing Ni complexes) was used as a pseudoreference electrode. Ferrocene was used as an internal standard, and all potentials were referenced to the ferrocenium/ferrocene (Cp$_2$Fe$^+$/Cp$_2$Fe) couple. Due to solubility limitations, the electrochemistry of nickel amino acid complexes was investigated in acetonitrile in the presence of 1.3 M water.

H$_2$ Production Measurements [Ni(P$_2$^{Ph}N$^{NNA\text{-}amino\ ester}$)$_2$]$^{2+}$. A 1.0 mL, 1 mM solution of the metal complex in acetonitrile containing 0.2 M Et$_4$N$^+$BF$_4$$^−$ was made. Metal complexes were titrated with acetonitrile solutions containing the triflic acid salt of protonated dimethylformamide (HDMF$^+$). The cathodic current (i_p) for the Ni$^{II/I}$ couple was recorded. Aliquots (10−20) of acid (2 M) were added via microsyringe in 10 μL increments until the catalytic current stopped increasing. At the end of the experiment, 4−7 aliquots of degassed water were added in 5 μL increments, until the catalytic current stopped increasing. The cathodic current (i_p) was corrected for dilution and the catalytic current (i_{cat}) was measured at −0.9 and −1.1 V. The ratios of i_{cat}/i_p versus the acid concentration were plotted, and the i_{cat}/i_p ratio in the acid independent region was used to determine the catalytic rate constant using the following equation:

$$\frac{i_{cat}}{i_p} = \frac{2}{0.4463}\sqrt{\frac{RTk[\text{H}^+]^2}{Fv}} \tag{1}$$

where R is the gas constant, T is the temperature in kelvin, F is the Faraday constant, v is the scan rate in volts per second, a one electron

process is assumed, and k is the observed rate constant.[25−28] Each measurement was repeated at least 3 times for statistical purposes.

H$_2$ Production Measurements [Ni(P$_2$^{Ph}N$^{NNA\text{-}amino\ acid}$)$_2$]$^{2+}$. The electrocatalysis experiments of the amino acid substituted nickel complexes were performed in a manner similar to that used for the amino ester substituted complexes, with a modification to account for the residual amount of trifluoroacetic acid introduced during cleavage of the complex from the resin. To obtain accurate i_p and i_{cat} values, a 200 μL, 0.5 mM solution of each metal complex containing 1.3 M water and 0.2 M Et$_4$N$^+$BF$_4$$^−$ was made in acetonitrile and the solution was divided into two fractions: one solution was used for the i_p measurement and the other was used for the i_{cat} measurements. To the first fraction, 50 μL of water and 850 μL of electrolyte solution were added. The additional water was added to this solution to maintain the solubility of the metal complexes after neutralization of the residual trifluoroacetic acid. The solution was titrated with 1 μL aliquots of 0.5 mM triethylamine solution until well-defined, fully reversible Ni$^{II/I}$ and Ni$^{I/0}$ couples were obtained. The cathodic current (i_p) was recorded for the Ni$^{II/I}$ couple by collecting the CV at a scan rate of 100 mV/s. In the second solution, 900 μL of electrolyte solution was added (the same total volume as was used in the experiments to determine i_p). This solution was titrated with acetonitrile solutions containing 2 M HDMF$^+$ (pK_a 6.1 in CH$_3$CN)[29] via microsyringe in 10 μL increments until the catalytic current stopped increasing. The cathodic current (i_p) in the absence of catalysis was corrected for dilution and the catalytic current (i_{cat}) at −0.9 and −1.1 V was measured. The ratios of i_{cat}/i_p versus the acid concentration were plotted, and the i_{cat}/i_p ratio in the acid concentration independent region was used to determine the catalytic rate using eq 1.

Determination of the Overpotential. The overpotential for the catalytic H$_2$ production using HDMF$^+$ as the acid source was calculated from the half-wave potential of the catalyst and the pK_a value of HDMF$^+$ using the method suggested by Evans and co-workers, with an $E^\circ_{H^+}$ = −140 mV.[30] E_{cat} is typically taken at the potential where leveling of the catalytic current occurs; however, since a clear leveling of the current was not observed for these complexes, the i_{cat} value was taken as −0.9 and −1.1 V. A representative figure illustrating where these potentials were chosen is given in the Supporting Information (Figure S3).

Determination of the Water Effect. In order to understand the impact of water on the rate of catalysis beyond the maximum catalytic current, electrocatalysis of the complex, $[Ni(P_2^{Ph}N^{NNA\text{-}Lys(Boc)OMe}_2)_2]^{2+}$, was performed in the presence of increasing concentrations of water. The catalyst containing solution was titrated with acetonitrile solutions containing HDMF$^+$ until the system had reached acid independence, as described above. To this solution, small aliquots (10 μL) of water were added and the catalytic current was measured after each addition, up to 7 M water.

■ RESULTS

Previously, we reported that the outer-coordination sphere plays an important role in modulating the H_2 production activity of $[Ni(P^R_2N^{R'}_2)_2]^{2+}$ catalysts.[22] In order to advance our understanding of the role of the outer-coordination sphere on catalytic activity, we have incorporated amino acids with acidic, basic, and neutral side chains (Table 1) into the parent complex, $[Ni(P^{Ph}_2N^{NNA}_2)_2]^{2+}$. The amino acids were coupled to $[Ni(P^{Ph}_2N^{NNA}_2)_2]^{2+}$ in order to make $[Ni(P^{Ph}_2N^{NNA\text{-}amino\ acid/ester}_2)_2]^{2+}$. The presence of the carboxylic acid groups in the parent complex, ($[Ni(P^{Ph}_2N^{NNA}_2)_2]^{2+}$), allows for the attachment of additional amino acids, while the presence of the phenyl substituent on nitrogen ensures the same electronic environment about the metal center as is found for the $[Ni(P^{Ph}_2N^{Ph}_2)_2]^{2+}$ complex, an active electrocatalyst for hydrogen production (720 s⁻¹).[13]

Synthesis and Characterization. *Ligands.* The coupling of amino acids to the ligand, $P^{Ph}_2N^{NNA}_2$, was achieved by using amino acids immobilized on a Wang resin, using DIC as a coupling reagent. The solid phase synthesis method prevents unwanted side reactions and easy removal of reaction byproducts (Scheme 1). Amino esters were coupled to $P^{Ph}_2N^{NNA}_2$ ligand using solution phase chemistry and 2-(1*H*-benzotriazol-1-yl)-1,1,3,3-tetramethyluronium tetrafluoroborate (TBTU) as a coupling reagent (Scheme 1). The reaction byproducts were removed by solvent extraction. The amino ester based ligands were prepared in reasonable yield (typically >50%) and good purity based on elemental analysis, mass spectrometry, 1D and 2D ^{1}H NMR, and ^{31}P{^{1}H} NMR. The ligands were found to be stable in air for short periods of time (1−2 days).

Metal Complexes. The $[Ni(P^{Ph}_2N^{NNA\text{-}amino\ ester}_2)_2](BF_4)_2$ complexes were prepared by addition of 2 equiv of the $P^{Ph}_2N^{NNA\text{-}amino\ ester}_2$ ligand to 1 equiv of $[Ni(CH_3CN)_6](BF_4)_2$ in acetonitrile. The metal complexes with amino acid ligands were prepared on resin in order to prevent decomposition of the ligand in the presence of TFA, used with TIS and water to cleave the product from the resin (Scheme 2). All of the metal

**Scheme 2. Synthesis of $[Ni(P^{Ph}_2N^{NNA\text{-}amino\ acid}_2)_2]^{2+}$ Complexes**[a]
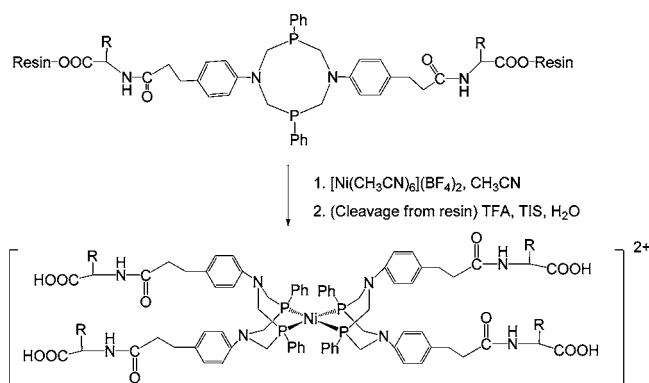
[a]Where R = amino acid side chain.

complexes were obtained in reasonable yield (∼80%) and good purity based on characterization using 1D and 2D ^{1}H NMR spectroscopy, 1D ^{31}P{^{1}H} NMR spectroscopy, and mass spectroscopy. The ^{1}H NH and αCH assignments for both ligands and metal complexes in acetonitrile are shown in Supporting Information Table S1. The metal complexes are

stable solids and are also stable in acetonitrile or acetonitrile:water mixtures, with slow decomposition in the presence of air.

^{31}P NMR Studies. The ^{31}P{^{1}H} NMR spectra of the amino ester containing nickel complexes at −40 °C display two symmetric resonances, as previously reported[19,22] and are consistent with slow exchange between the axial and equatorial phosphine atoms in the solvent bound, five coordinate structure (Figure 1). At room temperature, the ^{31}P{^{1}H} NMR spectra of
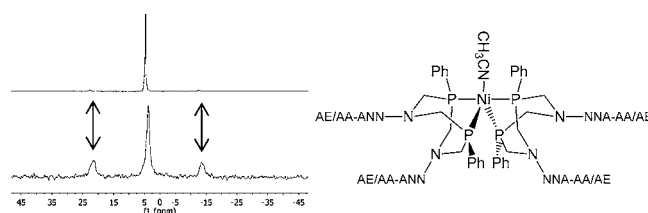

Figure 1. ^{31}P{^{1}H} NMR of the amino ester complex, $[Ni(P^{Ph}_2N^{NNA\text{-}Glu(OMe)OMe}_2)_2]^{2+}$, in CD$_3$CN (top spectrum) and the amino acid complex $[Ni(P^{Ph}_2N^{NNA\text{-}Ala}_2)_2]^{2+}$ in CD$_3$CN containing 6 M water (bottom spectrum) at room temperature. The symmetric resonances about the central resonance, indicated with arrows, are due to a portion of the five-coordinate complex (right) undergoing a slow exchange process which is only observed at reduced temperatures for complexes that are not substituted with amino acids/esters.

the amino ester substituted nickel complexes are very similar to the $[Ni(P^{Ph}_2N^{Ph}_2)_2]^{2+}$ complex, with a narrow singlet at 4−5 ppm (Figure 1, top). The narrow singlet is the result of fast structural exchange (reversible dissociation of the fifth ligand, acetonitrile, and subsequent structural rearrangement).[19] Upon closer inspection of the room temperature spectra, two small broad resonances, symmetric about the central resonance, at 21 and −13 ppm are also observed for all of the ester substituted nickel complexes. These resonances have identical chemical shifts to those of the low temperature spectrum. These additional resonances were observed previously for related nickel dipeptide complexes[22] and collectively, the three resonance were interpreted to be the result of a single complex, a portion of which is undergoing much slower structural reorganization due to intramolecular hydrogen bonding interactions.[22] However, the ^{31}P{^{1}H} spectra for the amino ester substituted nickel complexes show that very little of the complex has restricted motion, based on the low integrated intensity of the two symmetric resonances (<6%).

In contrast to the amino ester containing complexes, the amino acid containing complexes display more hindered motion, as evidenced by the increased integrated intensity in the two additional resonances about the central resonance (Figure 1, bottom). As observed by the ^{31}P{^{1}H} NMR spectra, almost 50% of the complex is influenced by restricted motion. The ^{31}P−^{31}P EXSY spectra of the complexes exhibit cross peaks between all three resonances (Supporting Information Figure S1), indicating that all three resonances are in exchange with each other, consistent with previously published results.[22] The observation of a larger population exhibiting restricted motion in the amino acid substituted nickel complexes relative to the esterified counterparts is thought to be due to stronger interactions between the carboxylate groups in the outer-coordination sphere.

Structural Dynamics of $[Ni(P^{Ph}_2N^{NNA\text{-}amino\ acid}_2)_2]^{2+}$ Complexes. The ability of the amino acid complexes to change protonation state may result in the differences observed in the dynamics compared to the analogous ester complexes. To

investigate this possibility, the amino acid complexes were investigated at varying solution pH values. The $^{31}P\{^1H\}$ NMR spectra were collected at pH = 1.0, 2.5, and 4.0 and displayed a strong dependence upon solution pH. At pH = 4.0, where 50–100% of the backbone and side chain carboxylic acid groups should be deprotonated, the $^{31}P\{^1H\}$ NMR spectra for the nickel complexes containing alanine, aspartic acid, and glutamic acid display all three resonances, indicative of restricted motion. The $^{31}P\{^1H\}$ spectra for $[Ni(P^{Ph}_2N^{NNA-Ala}_2)_2]^{2+}$ at pH = 4.0 is shown in Figure 2 (top) and demonstrates a larger degree of restricted
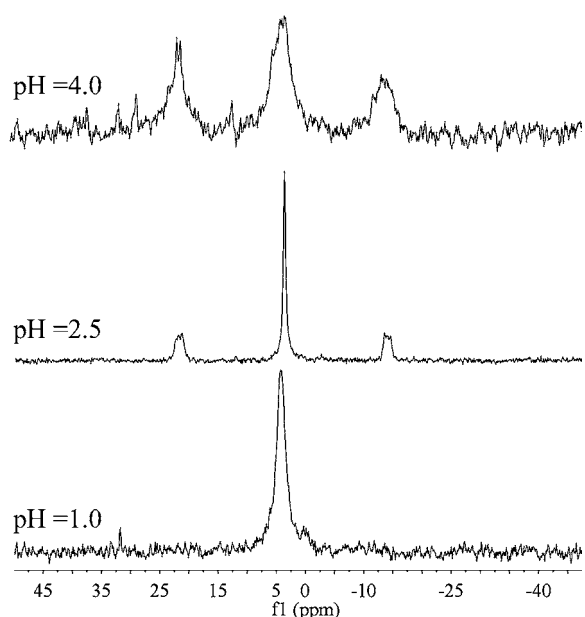
**Figure 2.** $^{31}P\{^1H\}$ NMR of 10 mM $[Ni(P^{Ph}_2N^{NNA-Ala}_2)_2]^{2+}$ complex at pH 4.0 (top spectrum), pH 2.5 (middle spectrum), and pH 1.0 (bottom spectrum). The spectra were collected at room temperature in CD₃CN containing 6 M water. The increase in integrated intensity in the symmetric resonances as a function of increased pH suggests that deprotonation of carboxylic acid groups in the outer-coordination sphere results in the reduced motional freedom observed in the amino acid containing nickel complexes.

motion than observed at pH = 2.5 (Figure 2, middle) based on the integrated intensity of the three resonances. Increased restricted motion as the complex is deprotonated could be due to charge repulsion between the deprotonated carboxylic acid groups in the amino acid leading to a more constrained geometry.

At a solution pH of 1.0, where full protonation of the side chains and backbone is expected, the resonances indicative of restricted motion disappear, indicating an increase in motional freedom when the side chains are protonated (Figure 2, bottom). This is a particularly important observation since under the highly acidic conditions which are used for catalysis, the structural rigidity is removed or significantly decreased, thereby allowing the twisting to a tetrahedral geometry which is required during the nickel(II/I) reduction in the catalytic cycle.[19] It was unexpected that the fully protonated complex would have less motional restriction, due to the expected increase in hydrogen bonding; however, the presence of water that is necessary for solubility would likely break up any intramolecular hydrogen bonding. Unfortunately, this hypothesis cannot be easily tested due to the lack of solubility of the amino acid containing complexes in the absence of water or strong acid. In summary,

the motional processes observed for the amino acid substituted nickel complexes are most consistent with a single complex exhibiting one or more exchange processes which are being influenced by the protonation state of the carboxylic acid groups in the side chains and backbone.

In contrast to the complexes that contain acidic amino acids, the basic amino acid containing lysine complex displayed only a central resonance, with no evidence of the additional resonances at pH = 1.0 or 3.5 (Figure 3). This is consistent with the
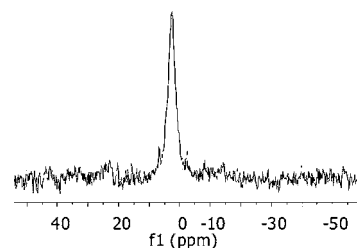
Figure 3. $^{31}P\{^1H\}$ NMR of $[Ni(P^{Ph}_2N^{NNA-Lys}_2)_2]^{2+}$ in CD₃CN containing 6.0 M water at room temperature and pH 1.0.

interpretation put forth above for the catalysts containing acidic amino acids, since the lysine side chain would be protonated during the entire pH range studied. Motional restriction is not observed for the lysine containing Ni complex likely due to the mixture of charges in the side chain (+) and the backbone (−) eliminating charge repulsion. Confirming this would require preparing a negatively charged complex, but the complex was not stable at the pH necessary for deprotonation of the lysine side chain (pK_a = 10−11).

Electrochemistry. *Cyclic Voltammetry Studies of [Ni-($P^{Ph}_2N^{NNA-amino\ acid/ester}_2)_2]^{2+}$ Complexes.* Each of the $[Ni-(P^{Ph}_2N^{NNA-amino\ acid/ester}_2)]^{2+}$ complexes display two distinct reversible reduction waves (i_a/i_c = 0.78−1.1) with a peak-to-peak separation (ΔE_p) for each of the waves of 70−92 mV (Table 2, Figure 4) in acetonitrile or acetonitrile/water mixtures. The two waves are assigned to the Ni(II/I) and Ni(I/0) couples, consistent with the previously reported complex, $[Ni-(P^{Ph}_2N^{NNA}_2)_2]^{2+}$ (Table 2).[14,18] All redox potentials are reported vs the Cp₂Fe$^{+/0}$ couple. Plots of the peak current (i_p) versus the square root of the scan rate display linear relationships for both couples indicating that these redox processes are diffusion controlled. Values of $E_{1/2}$ for the Ni(II/I) and Ni(I/0) couples range from −0.81 to −0.86 V and −0.96 to −1.04 V, respectively. The Ni(II/I) couples of the amino acid substituted nickel complexes occur at 20−30 mV more negative potential than the amino ester containing complexes, while the Ni(I/0) couples are similar for both. The cyclic voltammetry of $[Ni-(P^{Ph}_2N^{NNA-Lys}_2)_2]^{2+}$ was performed in the presence of 8.0 M water due to the limited solubility of this complex in acetonitrile containing 1.3 M water, which is used for the other amino acid substituted nickel catalysts. The Ni(II/I) and Ni(I/0) couple of $[Ni(P^{Ph}_2N^{NNA-Lys}_2)_2]^{2+}$ occurred at a more positive potential than the previously reported complex, $[Ni(P^{Ph}_2N^{NNA}_2)_2]^{2+}$, due to the presence of higher concentrations of water in the electrochemical cell. This was established by investigating the electrochemistry of $[Ni(P^{Ph}_2N^{NNA-Lys(Boc)OMe}_2)_2]^{2+}$ in dry acetonitrile and in acetonitrile containing 8 M water, where a similar shift in potentials was observed.

Catalytic Hydrogen Production. The $[Ni-(P^{Ph}_2N^{NNA-amino\ acid/ester}_2)_2]^{2+}$ complexes are active electrocatalysts for hydrogen production (Table 3, Figures 5 and S2

Table 2. Electrochemical Data for $[Ni(P^{Ph}_2N^{NNA\text{-}amino\ acid/ester}_2)_2]^{2+}$ Complexes in Acetonitrile

	(Ni$^{II/I}$)			(Ni$^{I/0}$)		
metal complex	$E_{1/2}$ (V)	ΔE_p (mV)	i_a/i_c	$E_{1/2}$ (V)	ΔE_p (mV)	i_a/i_c
$[Ni(P^{Ph}_2N^{NNA\text{-}AlaOEt}_2)_2]^{2+}$	−0.84	78	0.78	−1.04	63	0.95
$[Ni(P^{Ph}_2N^{NNA\text{-}Glu(OMe)OMe}_2)_2]^{2+}$	−0.83	90	0.86	−1.00	69	0.90
$[Ni(P^{Ph}_2N^{NNA\text{-}Lys(Boc)OMe}_2)_2]^{2+}$	−0.83	92	0.90	−1.05	67	0.80
$[Ni(P^{Ph}_2N^{NNA\text{-}Asp(OMe)OMe}_2)_2]^{2+}$	−0.84	85	0.85	−1.04	61	0.98
$[Ni(P^{Ph}_2N^{NNA\text{-}Ala}_2)_2]^{2+\ a}$	−0.85	70	0.80	−1.04	62	0.95
$[Ni(P^{Ph}_2N^{NNA\text{-}Glu}_2)_2]^{2+\ a}$	−0.86	90	0.85	−1.04	79	1.00
$[Ni(P^{Ph}_2N^{NNA\text{-}Lys}_2)_2]^{2+\ b}$	−0.81	82	1.10	−0.96	75	1.05
$[Ni(P^{Ph}_2N^{NNA\text{-}Asp}_2)_2]^{2+\ a}$	−0.86	87	0.85	−1.04	70	0.84

[a]Electrochemistry was performed in acetonitrile in the presence of 1.3 M water. [b]Electrochemistry was performed in the presence of 8 M water.
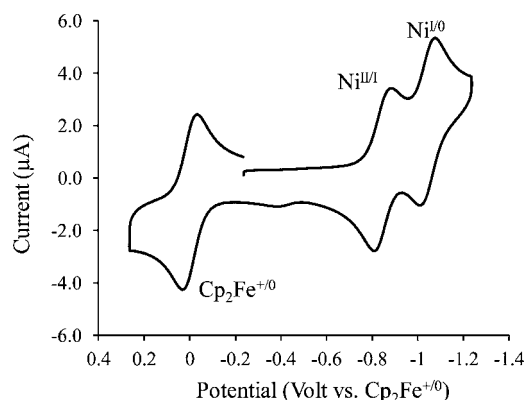

Figure 4. Cyclic voltammogram of $[Ni(P^{Ph}_2N^{NNA\text{-}AlaOEt}_2)_2]^{2+}$ in dry acetonitrile, typical of the voltammograms of nickel complexes containing either amino esters or amino acids. Conditions: 0.2 mM Et$_4$N$^+$BF$_4^-$ electrolyte, 1 mm glassy carbon working electrode, scan rate 500 mV/s. Ferrocene was used as an internal standard.

Table 3. Maximum Turnover Frequencies (TOF, s^{-1}) and Overpotentials (OP, mV) for Electrocatalytic Hydrogen Production by $[Ni(P^{Ph}_2N^{NNA\text{-}amino\ acid/ester}_2)_2]^{2+}$

$[Ni(P^{Ph}_2N^{NNA\text{-}amino\ acid/ester}_2)_2]^{2+}$	water conc. (M)	TOF (±25%) @ −0.9 V OP = ~320 mV	TOF (±25%) @ −1.1 V OP = ~ 420 mV
$[Ni(P^{Ph}_2N^{NNA\text{-}Lys}_2)_2]^{2+}$	1.30	1340	3350
$[Ni(P^{Ph}_2N^{NNA\text{-}Glu}_2)_2]^{2+}$	1.30	1300	3100
$[Ni(P^{Ph}_2N^{NNA\text{-}Asp}_2)_2]^{2+}$	1.30	1400	2600
$[Ni(P^{Ph}_2N^{NNA\text{-}Ala}_2)_2]^{2+}$	1.30	940	2600
$[Ni(P^{Ph}_2N^{NNA\text{-}Lys(Boc)OMe}_2)_2]^{2+}$	1.00	670	2000
$[Ni(P^{Ph}_2N^{NNA\text{-}GlyOEt}_2)_2]^{2+\ a}$	0.65	1400	1750
$[Ni(P^{Ph}_2N^{NNA\text{-}Asp(OMe)OMe}_2)_2]^{2+}$	0.85	630	1150
$[Ni(P^{Ph}_2N^{NNA\text{-}AlaOEt}_2)_2]^{2+}$	0.85	670	1100
$[Ni(P^{Ph}_2N^{NNA}_2)_2]^{2+\ a}$	0.65	900	970
$[Ni(P^{Ph}_2N^{NNA\text{-}Glu(OMe)OMe}_2)_2]^{2+}$	1.47	280	900
$[Ni(P^{Ph}_2N^{NNA\text{-}Gly}_2)_2]^{2+\ a}$	0.50	540	570
$[Ni(P^{Ph}_2N^{NNE}_2)_2]^{2+\ a}$	0.65	200	250

[a]Values taken from ref 22.

(Supporting Information). The electrocatalysis experiments on $[Ni(P^{Ph}_2N^{NNA\text{-}amino\ ester}_2)_2]^{2+}$ complexes were performed in dry CH$_3$CN using HDMF$^+$ as an acid source. The H$_2$ production activity was measured by cyclic voltammetry upon successive addition of acid until an acid concentration independent region was reached (Figure 5), after which the ratio i_{cat}/i_p remained constant, as shown in Figure 6. The observation of catalytic current enhancement at the Ni(II/I) couple demonstrates that catalysis proceeds with reduction of the Ni(II) complex followed

by protonation of the Ni(I) complex, consistent with the catalytic cycle proposed previously for catalysts of this class.[14] Due to the previous observation that water enhances catalysis,[13] water was added successively after the maximum current with acid was reached, until a new maximum current was reached. Due to solubility constraints, electrocatalysis of the amino acid substituted nickel complexes was performed in the presence of 1.3 M water and consequently, a water effect could not be established. Turnover frequencies were calculated using eq 1 and are shown in Table 3. These results show that the amino acid substituted nickel complexes display 2−4 fold higher rates than the corresponding amino ester substituted nickel complexes. Compared to the parent acid and ester complexes, $[Ni(P^{Ph}_2N^{NNA}_2)_2]^{2+}$ and $[Ni(P^{Ph}_2N^{NNE}_2)_2]^{2+}$, the rates of hydrogen production of the newly reported complexes are as much as 13 times faster.

While the rates for the complexes reported here are faster than those previously reported, the overpotential needed to achieve these rates is higher than for other complexes of this type (~420 vs ~300 mV for most previous complexes). The higher potential needed to drive these catalysts could indicate a slower rate of electron transfer or proton transfer than that observed for the unsubstituted $[Ni(P^{Ph}_2N^{Ph}_2)_2]^{2+}$ complex. The determination of the source of the higher overpotential is outside the scope of this work, but to allow direct comparison to previously published data, the rates are reported at two potentials: the potential used previously for the simpler amino acid and dipeptide substituted nickel complexes,[22] consistent with catalysis at the Ni(II/I) couple (−0.9 V), and at the highest current within the measured potential window, −1.1 V (Table 3 and Figure S3 (Supporting Information)). The current continues to increase beyond −1.1 V; however, quantification of the catalytic rates at potentials negative of −1.1 V is unreliable due to the reduction of protons at the glassy carbon electrode, as well as apparent electrode fouling.

Effect of Solvent Composition on Catalytic Rates. Electrocatalytic studies in acetonitrile display an increase in catalytic current upon addition of water to the catalytic reaction mixture (after reaching the acid independent region), consistent with previous observations.[13,22] However, after the maximum increase in current enhancement was reached by adding water, further addition of water resulted in a substantial decrease in catalytic current. Figure 7 shows the behavior of the observed catalytic rate of the complex $[Ni(P^{Ph}_2N^{NNA\text{-}Lys(Boc)OMe}_2)_2]^{2+}$ as a function of water concentration.

Although the amino acid substituted nickel complexes cannot be studied in the absence of water, the catalytic rates in the presence of 10 M water were found to be lower than the rates in the presence of 1.3 M water. In order to test if this was due to the inability to reach acid concentration independence in these
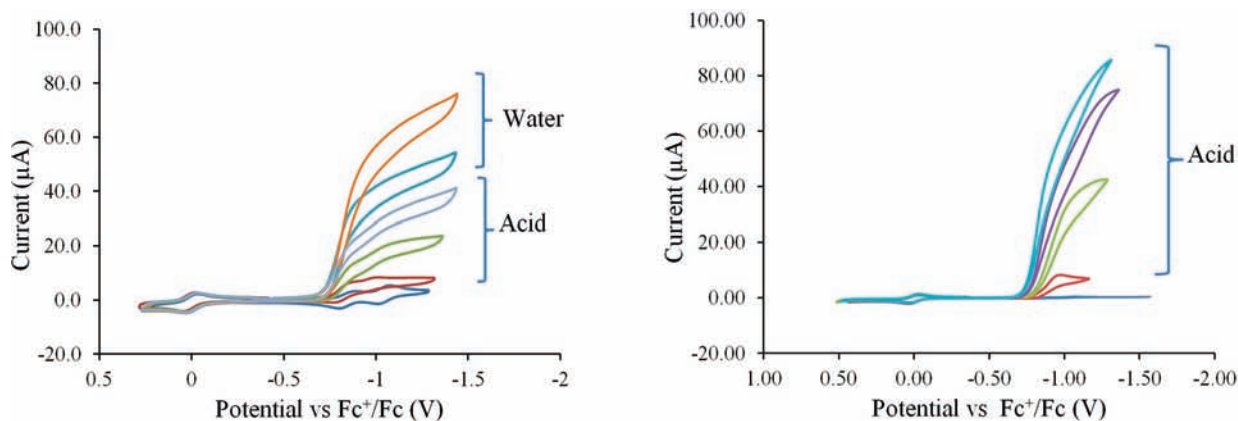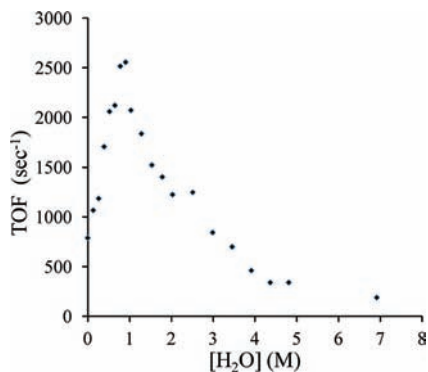
Figure 5. Successive cyclic voltammograms of the amino acid and amino ester containing complexes as a function of increasing acid (HDMF$^+$) concentration. (left) $[Ni(P^{Ph}_2N^{NNA-Asp(OMe)OMe}_2)_2]^{2+}$ in dry acetonitrile at a scan rate of 500 mV/s. (right) $[Ni(P^{Ph}_2N^{NNA-Asp}_2)_2]^{2+}$ in acetonitrile containing 1.3 M water at a scan rate of 100 mV/s. Conditions: 0.2 mM Et$_4$N$^+$BF$_4^-$ electrolyte, 1 mm glassy carbon working electrode. Ferrocene was used as an internal standard.
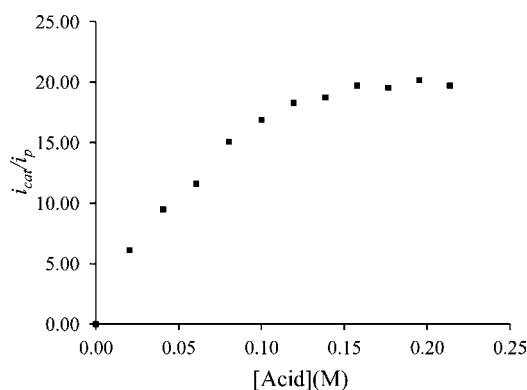
Figure 6. Plot of the ratio of the catalytic current (i_{cat}) to the peak current of the Ni$^{II/I}$ couple in the absence of the acid (i_p) versus the concentration of HDMF$^+$ in dry acetonitrile. Conditions: 500 mV/scan rate, 0.2 M Et$_4$N$^+$BF$_4^-$ in dry acetonitrile, 1 mM complex [Ni-(P$^{Ph}_2$N$^{NNA-Lys(Boc)OMe}_2)_2]^{2+}$, glassy carbon electrode.

experiments, electrocatalysis of all four of the amino acid substituted nickel complexes was performed at 10 M water using HDMF$^+$ as the acid source. The acid concentration independent region was attained suggesting that protonation of the catalyst

was not rate limiting, but the H$_2$ production rates were decreased by 30-fold compared to studies with 1.3 M water. To verify that the reduction of catalytic rates was not due to the change in solution pH under conditions of high water concentration, catalysis was performed using a stronger acid (triflic acid, pK_a = 2.6 in CH$_3$CN)[29] in the presence of 10 M water. Again, an acid independent region was reached, and reduced rates were also observed (∼10−20 fold slower with 10 M water), indicating that reduction in catalytic rate is not due to a change in solution pH.

Because of the strong dependence of catalytic rate on water concentration, an additional experiment was undertaken to ensure that the use of 1.3 M water in measuring catalysis for the amino acid substituted nickel complexes was optimal (the peak maximum in Figure 7) and was not limiting the measured catalytic rates. While insoluble in dry acetonitrile alone, the alanine substituted nickel complex is soluble in dry acetonitrile in the presence of acid. Sufficient acid to achieve acid concentration independence was added, followed by the sequential addition of water. An increase in catalytic current was observed up to 1.0 M water, at which concentration, the current began to decrease. However, the maximum catalytic current was only slightly larger at water concentrations of 1.0 M than for 1.3 M water; therefore, the rates in Table 3 are the fastest catalytic rates achievable for the amino acid containing catalysts, within the accuracy of the experiment.

Figure 7. Turnover frequency (s^{-1}) of $[Ni(P^{Ph}_2N^{NNA-Lys(Boc)OMe}_2)_2]^{2+}$ (1 mM) as a function of water concentration using $[HDMF]^+$ as the acid source in acetonitrile containing 0.2 M Et$_4$N$^+$BF$_4^-$. Initially water enhances the rate of catalysis, but after the maximum concentration is reached, further additions of water decrease the rate dramatically.

DISCUSSION

Molecular mimics of hydrogenase enzymes have provided important mechanistic insight into the enzyme by studying the effects of, and optimizing, the first and second coordination spheres, resulting in rates surpassing both Ni−Fe and Fe−Fe hydrogenases, albeit at higher overpotentials.[10−14,18−22] The outer-coordination sphere has also been shown to influence catalysis. For instance, the addition of water provides a 2−70 fold increase in rate, where water was proposed to enhance proton movement.[13,22] Another example includes the use of ionic liquids, in which the catalytic rates have been shown to increase by nearly 2 orders of magnitude.[31] Neither of these contributions appears to be due to direct interaction with the metal and therefore is best proposed to occur in the outer-coordination sphere.

In an effort to incorporate these outer-coordination features as an integral part of the catalyst, we began by investigating a series

of amino acid and dipeptide substituted nickel complexes. These initial studies showed that introducing amino acids into the outer-coordination sphere of $[Ni(P^{Ph}_2N^{Ph}_2)_2]^{2+}$ catalysts can result in modulating the catalytic activity of molecular hydrogenase mimics by nearly an order of magnitude.[22] Before a more complex outer-coordination sphere can be added, the role of individual amino acids within the nickel dipeptide catalysts needs to be understood. By investigating acidic, basic, and neutral amino acids and their corresponding esters, we have investigated the roles of sterics, the ability to protonate the side chain and the pK_a of the amino acid side chain on the rate of catalysis without significantly changing the first and second coordination spheres. This work provides important advancements in our understanding of the role of the outer-coordination sphere on catalytic activity. (1) Higher catalytic rates are observed with amino acid substituted nickel complexes containing acidic and basic amino acids than complexes containing neutral amino acids or amino esters, suggesting that the protonation of the amino acid side chains plays an important role in contributing to catalytic activity. (2) Higher rates with larger complexes confirm that catalytic activity is not limited by steric constraints. Notably, one of the largest catalysts, $[Ni(P^{Ph}_2N^{NNA-Lys}_2)_2]^{2+}$ displays the fastest rate.

The catalytic rates for $[Ni(P^{Ph}_2N^{NNA-amino\ acid/ester}_2)_2]^{2+}$ complexes display turnover frequencies for hydrogen production ranging from 200 to 1400 s^{-1} at an overpotential of ∼0.32 V and from 250 to 3350 at an overpotential of ∼0.42 V, some of the fastest rates reported for these complexes in acetonitrile to date. General trends are consistent at both overpotentials. The amino acid substituted nickel complexes display faster rates than the corresponding amino ester substituted nickel complexes. The ensuing discussion will focus on making direct comparisons of the measurements at the higher overpotential.

H₂ Production Rates of Amino Acid Substituted Nickel Complexes. Amino acid substituted nickel complexes display higher rates for hydrogen production compared to the corresponding amino ester containing complexes, and 2−4 times that of the parent complex, $[Ni(P^{Ph}_2N^{NNA}_2)_2]^{2+}$. The largest complex, $[Ni(P^{Ph}_2N^{NNA-Lys}_2)_2]^{2+}$, displays the highest rate of H₂ production, 3350 s^{-1}. Indeed, the rates of the amino acid substituted nickel complexes increase with increasing complex size indicating that steric inhibition does not dominate catalytic activity.

The increase in rate with increasing size was somewhat surprising, since the catalyst undergoes a structural rearrangement from square planar to tetrahedral during the transformation from Ni(II) to Ni(0) in the catalytic cycle,[18−20] a process which could be hindered by bulky substituents which also have the potential to interact intramolecularly, interactions which would render structural rearrangement even more difficult. NMR evidence of the Ni(II) complex suggested that the amino acid substituted nickel complexes had restricted motional processes likely due to charge repulsion at pH 3−4, but under catalytic conditions (pH < 1), where the catalyst was fully protonated, these interactions were significantly reduced. While the NMR and electrocatalytic experiments are not directly comparable, the NMR experiment does provide evidence that under catalytic conditions, intramolecular interactions causing slow structural exchange are minimized.

Catalytic Rates of Neutral and Charged Amino Acid Substituted Nickel Complexes. Nickel complexes containing amino acids with acidic or basic side chains (Asp, Glu, Lys) display higher rates of hydrogen production compared to neutral amino acids (Gly, Ala). The lysine containing complex,

$[Ni(P^{Ph}_2N^{NNA-Lys}_2)_2]^{2+}$, is 1.3 and 5.8 times faster than the alanine and glycine containing complexes, respectively, and the glutamic acid containing complex, $[Ni(P^{Ph}_2N^{NNA-Glu}_2)_2]^{2+}$, displays 1.2 and 5.4 times faster rates of hydrogen production than the alanine and glycine containing metal complexes. This could be due to the larger number of sites for protonation in the catalysts with acidic and basic side chains.

The aspartic acid containing complex, $[Ni(P^{Ph}_2N^{NNA-Asp}_2)_2]^{2+}$, exhibits a slightly slower rate of H₂ production than the glutamic acid containing complex. The small but significant difference in these two complexes is surprising in the case of molecular catalysts. Glutamic acid and aspartic acid substitutions in proteins often result in dramatic effects in function. For instance, Hegg and co-workers have shown that the substitution of glutamic acid by aspartic acid results in a drastic reduction in hydrogenase activity relative to the native enzyme.[32] This is thought to be due to a specific placement of the side chain that is accommodated by the increased chain length in glutamic acid, but in the amino acid complexes prepared here, $[Ni(P^{Ph}_2N^{NNA-amino\ acid}_2)_2]^{2+}$, there is no evidence for the amino acids being positioned in a unique location. Specifically, the ligands in these molecular catalysts have few structural restrictions and are likely experiencing large fluctuations preventing a specific interaction such as that observed in enzymes. Although the difference in rates of the complexes $[Ni(P^{Ph}_2N^{NNA-Asp}_2)_2]^{2+}$ and $[Ni(P^{Ph}_2N^{NNA-Glu}_2)_2]^{2+}$ is marginally outside of the error for those two experiments, it is an interesting observation that may warrant future consideration.

Rates for Amino Ester Substituted Nickel Complexes. The amino ester substituted nickel complexes display up to four times lower rates of hydrogen production compared to the amino acid substituted nickel complexes, with rates from 250 to 2000 s^{-1}. Similar to the amino acid substituted nickel complexes, the amino ester substituted nickel complexes require a higher overpotential to achieve their fastest rates, and at these more negative potentials, all of the amino ester substituted catalysts display faster rates of H₂ production than the parent ester complex, $[Ni(P^{Ph}_2N^{NNE}_2)_2]^{2+}$. Similar to the amino acid substituted nickel complexes, the correlation between rate and size is opposite of the expected trend, since $[Ni(P^{Ph}_2N^{NNA-Lys(Boc)OMe}_2)_2]^{2+}$ is the largest and fastest amino ester substituted catalyst, and $[Ni(P^{Ph}_2N^{NNE}_2)_2]^{2+}$ is the smallest and slowest. The slower rates observed for the amino ester substituted complexes may be related to the inability of these functional groups to protonate, unlike the nonesterified equivalents in the amino acid substituted complexes. Protonation of or hydrogen bonding to the functional groups found in the amino acid substituted nickel complexes could result in facilitating proton transfer due to the higher local concentration of protons from both the protonated side chains (COOH and NH₃⁺) and backbone (COOH) functional groups. Esterification removes this functionality, thereby providing an opportunity for both study and control.

Water Effect. In the presence of water, the amino ester substituted nickel complexes display 2−3 fold increases in the rates of hydrogen production compared to only a 1.3 fold increase observed for the parent complexes, $[Ni(P^{Ph}_2N^{NNA}_2)_2]^{2+}$ or $[Ni(P^{Ph}_2N^{NNE}_2)_2]^{2+}$.[22] An unusually large water effect was also observed for the analogous complex, $[Ni(P^{Ph}_2N^{Ph-P(O)(OEt)2}_2)_2]^{2+}$ and for complexes with bulky substituents on phosphine which can block the access to the pendant amine.[13,33] In this case, the substituent on the phosphorus is constant, but it is possible that the ester substituted complexes create steric bulk which blocks access to the active site. While crystal structures have not yet

been obtained, they may, along with computational modeling, provide insight into the unusually large effect of water observed here.

Although we were not able to obtain the effect of water on the rates for the amino acid substituted nickel complexes due to the insolubility of these complexes in the absence of water, the fast rates obtained for these catalysts are likely a result of the presence of water. In addition to the potential ability of the amino acid substituted nickel complexes to provide higher local concentrations of protons, discussed above, they may also be capable of concentrating water, which is known to enhance catalysis. Concentration is a method used by enzymes to enhance catalytic rates and it may be that the $[Ni(P^{Ph}_2N^{NNA\text{-}amino\ acid}_2)_2]^{2+}$ complexes display the same mechanism.

While water was observed to enhance catalytic rates at low to moderate concentrations, initial rates measured for the amino acid substituted nickel complexes in 10 M water yielded rates that were only ∼3% of the rates observed in the presence of 1.3 M water. These results are consistent with the dramatic decrease in the catalytic rates that were observed for the complex $[Ni(P^{Ph}_2N^{NNA\text{-}Lys(Boc)OMe}_2)_2]^{2+}$ once the optimal water concentration (∼1.3 M) had been exceeded. The observation that an acid concentration independent region is obtained, even with this large concentration of water, shows that the decrease in rate at high concentrations of water is not merely due to a change in pH of the solution, or through the stabilization of protons through solvation by water to form H_3O^+ and higher hydrates. In addition, if the slower rates were due to a rise in the pH, a stronger acid would be expected to produce higher catalytic rates. However, electrocatalysis in the presence of triflic acid with 10 M water was also found to have substantially lower rates (by a factor of 10−20). This result does suggest that water has multiple roles, some of which are beneficial to catalysis and some of which hinder catalysis, possibly by alterations in hydrogen bonding interactions at varying water concentrations. The role of water in electrocatalytic hydrogen production of $[Ni(P^R_2N^{R'}_2)_2]^{2+}$ complexes is currently under investigation.

Mechanistic Insight. The effects observed here, far from the active site, and isolated to the outer-coordination sphere are remarkable. The rates of the catalysts can be modified by over an order of magnitude, with relatively subtle changes, and can enhance the rate of the unmodified complex by ∼5 times. These effects are reminiscent of the effects observed in enzymes and emphasize the importance of a protein scaffold in the development of molecular catalysts. An important difference in the catalysts reported here is that the functional groups are not constrained by a well-defined protein scaffold and therefore the observed effects are best explained as global features, such as increasing the concentration of protons near the active site. The local effects achieved by precise positioning can be tested with the introduction of a structured outer-coordination sphere, the topic of future study.

SUMMARY

These studies show that the catalytic activity of molecular hydrogenase mimics can be tuned by modifications in the outer-coordination sphere. Acidic, basic, and neutral amino acids and the corresponding amino esters were incorporated into complexes having the general formula $[Ni(P^{Ph}_2N^{NNA\text{-}amino\ acid/ester}_2)_2]^{2+}$ allowing the investigation of the role of side chain pK_a, the ability to protonate the side chain/backbone, and sterics on the rate of hydrogen production. The

amino acid substituted nickel complexes display 2−4 times higher rates of hydrogen production than the corresponding ester complexes, providing evidence that protonation of carboxylic acid and amine groups plays an important role in catalytic H_2 production, possibly by facilitating proton transfer to the active site or increasing proton concentration near the active site. Rates were faster for larger complexes demonstrating that catalytic activity is not hindered by large ligand sizes. The order of magnitude change in rates with this series of complexes allows for the tuning of catalytic activity without significantly modifying the active site and signifies the influence that a well-designed outer-coordination sphere can have on the rate of catalysis.

■ ASSOCIATED CONTENT

⑤ Supporting Information

Table S1 and Figures S1−S3 as mentioned in the text. This material is available free of charge via the Internet at http://pubs.acs.org.

■ AUTHOR INFORMATION

Corresponding Author
*E-mail: wendy.shaw@pnnl.gov.

Notes
The authors declare no competing financial interest.

■ ACKNOWLEDGMENTS

■ REFERENCES

(1) Fontecilla-Camps, J. C.; Volbeda, A.; Cavazza, C.; Nicolet, Y. *Chem. Rev.* **2007**, *107*, 4273.

(2) Frey, M. *ChemBioChem* **2002**, *3*, 153.

(3) Nicolet, Y.; de Lacey, A. L.; Vernede, X.; Fernandez, V. M.; Hatchikian, E. C.; Fontecilla-Camps, J. C. *J. Am. Chem. Soc.* **2001**, *123*, 1596.

(4) Peters, J. W.; Lanzilotta, W. N.; Lemon, B. J.; Seefeldt, L. C. *Science* **1998**, *282*, 1853.

(5) Shima, S.; Pilak, O.; Vogt, S.; Schick, M.; Stagni, M. S.; Meyer-Klaucke, W.; Warkentin, W.; Thauer, R. K.; Ermler, U. *Science* **2008**, *321*, 572.

(6) Silakov, A.; Wenk, B.; Reijerse, E.; Lubitz, W. *Phys. Chem. Chem. Phys.* **2009**, *11*, 6592.

(7) Curtis, C. J.; Miedaner, A.; Ciancanelli, R.; Ellis, W. W.; Noll, B. C.; Rakowski DuBois, M.; DuBois, D. L. *Inorg. Chem.* **2003**, *42*, 216.

(8) Fraze, K.; Wilson, A. D.; Appel, A. M.; Rakowski DuBois, M.; DuBois, D. L. *Organometallics* **2007**, *26*, 3918.

(9) Gloaguen, F.; Rauchfuss, T. B. *Chem. Soc. Rev.* **2009**, *38*, 100.

(10) Helm, M. L.; Stewart, M. P.; Bullock, R. M.; DuBois, M. R.; DuBois, D. L. *Science* **2011**, *333*, 863.

(11) Jacobsen, G. M.; Shoemaker, R. K.; McNevin, M. J.; Rakowski DuBois, M.; DuBois, D. L. *Organometallics* **2007**, *26*, 5003.

(12) Jacobsen, G. M.; Yang, J. Y.; Twamley, B.; Wilson, Aaron D.; Bullock, Morris; Rakowski DuBois, M.; DuBois, D. L. *Energy Environ. Sci.* **2008**, *1*, 167.

(13) Kilgore, U. J.; Roberts, J. A. S.; Pool, D. H.; Appel, A. M.; Stewart, M. P.; Rakowski DuBois, M.; Dougherty, W. G.; Kassel, W. S.; Bullock, R. M.; DuBois, D. L. *J. Am. Chem. Soc.* **2011**, *133*, 5861.

(14) Pool, D. H.; DuBois, D. L. *J. Organomet. Chem.* **2009**, *694*, 2858.

(15) Rakowski DuBois, M.; DuBois, D. L. *Chem. Soc. Rev.* **2009**, *38*, 62.

(16) Tard, C. d.; Pickett, C. J. *Chem. Rev.* **2009**, *109*, 2245.

(17) Volbeda, A.; Garcin, E.; Piras, C.; de Lacey, A. L.; Fernandez, V. M.; Hatchikian, E. C.; Frey, M.; Fontecilla-Camps, J. C. *J. Am. Chem. Soc.* **1996**, *118*, 12989.

(18) Wilson, A. D.; Fraze, K.; Twamley, B.; Miller, S. M.; DuBois, D. L.; Rakowski DuBois, M. *J. Am. Chem. Soc.* **2008**, *130*, 1061.

(19) Wilson, A. D.; Newell, R. H.; McNevin, M. J.; Muckerman, J. T.; Rakowski DuBois, M.; DuBois, D. L. *J. Am. Chem. Soc.* **2006**, *128*, 358.

(20) Wilson, A. D.; Shoemaker, R. K.; Miedaner, A.; Muckerman, J. T.; DuBois, D. L.; Rakowski DuBois, M. *Proc. Natl. Acad. Sci. U.S.A.* **2007**, *104*, 6951.

(21) Yang, J. Y.; Bullock, R. M.; Shaw, W. J.; Twamley, B.; Fraze, K.; Rakowski DuBois, M.; DuBois, D. L. *J. Am. Chem. Soc.* **2009**, *131*, 5935.

(22) Jain, A.; Lense, S.; Linehan, J. C.; Raugei, S.; Cho, H.; DuBois, D. L.; Shaw, W. J. *Inorg. Chem.* **2011**, *50*, 4073.

(23) Favier, I. D. E. *Tetrahederon Lett* **2004**, *45*, 3393.

(24) Hathaway, B. J. H., D. D.; Underhill, A. E. *J. Am. Chem. Soc.* **1962**, 2444.

(25) Delehay, P. S., G. L. *J. Am. Chem. Soc.* **1952**, *74*, 3500.

(26) Nicholson, R. S. S., I. *Anal. Chem.* **1964**, *36*, 706.

(27) Saveant, J. M. V., E. *Electrochim. Acta* **1965**, *10*, 905.

(28) Saveant, J. M. V., E. *Electrochim. Acta* **1967**, *12*, 629.

(29) Izutsu, K. *Acid-Base Dissociation Constants in Dipolar Aprotic Solvents*; Blackwell Scientific Publications: Oxford, 1990.

(30) Felton, G. A. N.; Glass, R. S.; Lichtenberger, D. L.; Evans, D. H. *Inorg. Chem.* **2006**, *45*, 9181.

(31) Pool, D. H.; Stewart, M. P.; O'Hagan, M.; Shaw, W. J.; Roberts, J. A. S.; Bullock, R. M.; DuBois, D. L. *Proc. Natl. Acad. Sci. USA* **2012**, DOI: 10.1073/pnas.1120208109.

(32) Cornish, A.; Gartner, K.; Yang, H.; Peters, J.; Hegg, E. *J. Biol. Chem.* **2011**, *286*, 38341.

(33) Kilgore, U. J.; Stewart, M. P.; Helm, M. L.; Dougherty, W. G.; Kassel, W. S.; Rakowski DuBois, M.; Dubois, D. L.; Bullock, R. M. *Inorg. Chem.* **2011**, *50*, 10908.